A Novel Discrete-Time Predictive Current Control for PMSM

Jung-Won Sun*, Jin-Woo Lee*, Jin-Ho Suh*, Young-Jin Lee**, and Kwon-Soon Lee***

* Department of Electrical Engineering, Dong-A University
840, Hadan-dong, Saha-gu, Busan, 604-714, Korea
Selove783@hanmail.net , suhgang@hanmail.net
** Dept. of Electrical Instrument and Control, Korea Aviation Polytechnic College
438 Egeum-dong, Sachon City, Kyungnam, 664-180, Korea
airlee@kopo.or.kr
*** Division of Electrical, Electronic, and Computer Eng., Dong-A University
840, Hadan-dong, Saha-gu, Busan, 604-714, Korea
kslee@daunet.donga.ac.kr

Abstract: In this paper, we propose a new discrete-time predictive current controller for a PMSM(Permanent Magnet Synchronous Motor). The main objectives of the current controllers are to ensure that the measured stator currents tract the command values accurately and to shorten the transient interval as much as possible, in order to obtain high-performance of ac drive system. The conventional predictive current controller is hard to implement in full digital current controller since a finite calculation time causes a delay between the current sensing time and the time that it takes to apply the voltage to motor. A new control strategy in this paper is seen the scheme that gets the fast adaptation of transient current change, the fast transient response tracking. Moreover, the validity of the proposed method is demonstrated by numerical simulations and the simulation results will present the improvements of predictive controller and accuracy of the current controller.

Keywords: PMSM, Predictive Current Control, SVPWM, Full digital System

1. INTRODUCTION

The main objectives of the current controller are to ensure that the measured stator currents track the required values accurately and to shorten the transient interval as much as possible. Until the present, various current controllers are proposed. Like the following those, generally, we classify into the four main type of current control schemes [1][2].

(1) *Hysteresis Control*: The hysteresis current control method has advantages such as a fast transient response and simple circuits in implementation. But it shows high and non-constant switching frequency inthe inverter. By the result, it generates the harmonics and reduces the length of circuit.
(2) *Ramp Comparison Control*: The Ramp Comparison Current Control method has the advantages of limiting the maximum inverter switching frequency and producing well-defined harmonics. Even though the controller has optimized gains, there are magnitude and phase delay errors in steady state since the control method has low pass filter characteristics.
(3) *Synchronous Frame Proportional Integer Control*: In addition to the rotor synchronous frame PI control, compensation of the back EMF and cross-coupling terms gives fast transient response and zero steady-state error irrespective of operating conditions.
(4) *Predictive Control*: In the predictive control scheme, the switching duties of the inverter switches are determined by calculating the required voltages forcing the motor phase currents to follow corresponding references. If the motor and inverter parameters are well known, the predictive controller shows the fast transient response and no steady state error. But If we do not know those, the predictive current controller is not implemented well.

With the development of microprocessor technology, most current control schemes can be implemented in full digital systems.

The purpose of this paper is to present a new predictive current control scheme based on a discretized model of the PMSM. In both transient and steady states, the proposed controller performs better than the conventional predictive controller does in a full digital control system. In the implementation of the controller, the effect of rotor position difference, voltage limitation are discussed and compensated. The simulation results are also presented to prove the feasibility and effectiveness of the proposed predictive current controller using a prototype 2.2 Kw PMSM servo drive system.

2. SYSTEM DESCRIPTION

2.1 Permanent Magnet Synchronous Motor

The equivalent circuit of PMSM shows in Fig. 1.

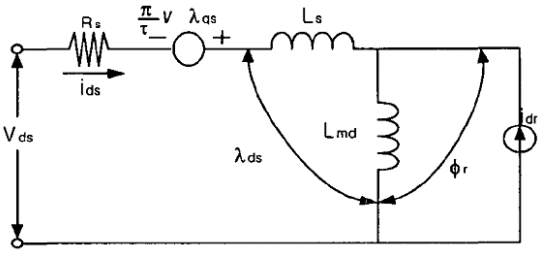

(a) d-axis circuit

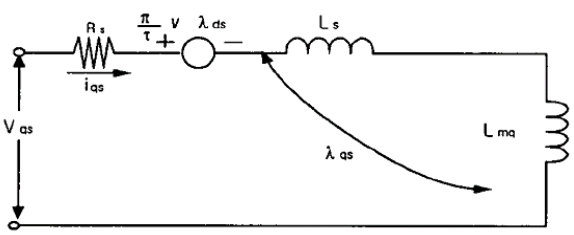

(b) q-axis circuit

Fig. 1 The equivalent circuit of PMSM

In the Fig. 1, the motor losses (copper, core, and mechanical), magnet saturation, air gap space harmonics and harmonic components of voltage and current are neglected in order to simplify the analysis.

In order to simulate, the voltage equation of PMSM in the synchronous reference can be expressed as follows:

$$V_{ds} = R_s i_{ds} + p\lambda_{ds} - \omega_r \lambda_{qs} \quad (1)$$

$$V_{qs} = R_s i_{qs} + p\lambda_{qs} + \omega_r \lambda_{ds} \quad (2)$$

with

$$\omega_e = n_p w_r$$

$$\lambda_{qs} = (L_s + L_{mq})\, i_{qs}$$

$$\lambda_{ds} = (L_s + L_{md})\, i_{ds} + \varphi_r$$

where

i_{ds}, i_{qs} : d-q axis current ;

V_{ds}, V_{qs} : d-q axis voltage ;

ϕ_r : flux linkage due to permanent magnet per phase ;

R_s : resistance of primary ;

L_s : self-inductance of primary ;

L_{md}, L_{mq} : d-q axis component of magnetizing inductance ;

ρ : d/dt ;

ω_e : electrical angular velocity ;

τ : pole pitch ;

ν : velocity ;

If the voltage equation is arranged, the equation can be expressed as follows [4].

$$V_{ds} = R_s i_{ds} + L_q \frac{d}{dt} i_{ds} - L_q i_{qs} w_e \quad (3)$$

$$V_{qs} = R_s i_{qs} + L_d \frac{d}{dt} i_{qs} + L_q w_e + \phi_{PM} \quad (4)$$

From the above voltage equation, the discrete-model voltage equation of a PM Synchronous Motor is described as follows.

$$V_{qs} = R_s i_{qs}(k) + \frac{L_q}{T_s}(i_{qs}(k+1) - i_{qs}(k)) + L_d \omega_e i_{ds}(k) + \phi_{PM}\omega_e \quad (5)$$

$$V_{ds} = R_s i_{ds}(k) + \frac{L_d}{T_s}(i_{ds}(k+1) - i_{ds}(k)) - L_q i_{qs}(k)\omega_e \quad (6)$$

where

T_s : sampling time ;

This equation is the discrete-model voltage equation of conventional predictive current controller

2.2 System of the motor drive

The component of the full digital servo drive system is presented as Fig. 2. The system is consisted of the three parts. The first is Speed controller. The second is current controller. The third is inverter.

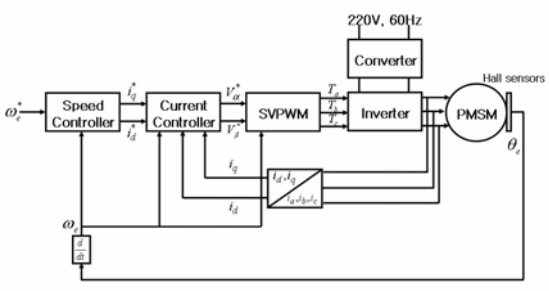

Fig. 1 Full System of the driver for PMSM

2.3 Space Vector PWM

The voltage space vector corresponding to eight switching states of the inverter are shown in Fig. 2. The section of the voltage space vector is divided into six sections. And the magnitude of each voltage vector that corresponds to six active states is 2/3 Vdc, and these vectors form a hexagon. And the voltage vectors u_0 and u_7 that correspond to freewheeling states are zero voltage vectors.

The Relation between voltage space vector and voltage commands in dq-axes is shown in Fig. 3. The V_{dc} is the dc link voltage, and the V_s is the magnitude of the space V_s. The V_s of voltage commands is calculated from the V_d^*, V_q^*, and θ_e.

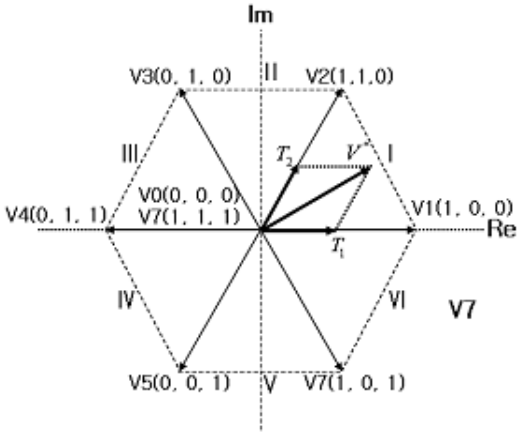

Fig. 2 Switching Voltage vectors of the three-phase inverter

In order to perform the SV-PWM(Space Vector Pulse Width Modulation), we need the following sequence. Here, we will discuss the I Section.

In the first time, we must select where the command voltage is existed. If the command voltage is putted in the I section, it is that satisfy as followings or if it don't satisfy the followings, command voltage is in the other section. And it must find a satisfactory section, immediately.

$$V_{\beta s}^* > 0 \quad \text{and} \quad \sqrt{3}\, V_{\alpha s}^* - V_{\beta s}^* > 0 \quad (7)$$

Next time, the decision of switching time is as follows:

$$T1 = \frac{\sqrt{3}T_s}{V_{dc}}\left(\frac{\sqrt{3}}{2}V_{\alpha s}^* - \frac{1}{2}V_{\beta s}^*\right) \quad (8)$$

$$T2 = \frac{\sqrt{3}T_s}{V_{dc}}\left(V_{\beta s}^*\right) \quad (9)$$

$$T3 = T_s - (T1 + T2) \quad (10)$$

And, the switching function of the I section is described as Table 1. The symmetrical switching function has various advantages. Especially, in the inverter, the scheme of PWM is important elements of PMSM, because the scheme affects the inverter deeply.

Various PWM schemes have been proposed. But the SP-PWM is known as a good scheme for a response of transient current controller. This has advantages of much scopes of linear control, the disturbance of low harmonics, and the response of rapid transient.

Table 1 The switching function of section I

Section	Switching Function	On mode			Off mode		
		$\frac{T_0}{2}$	$T1$	$T2$	$\frac{T_0}{2}$	$T1$	$T2$
Section I	T_a	1	0	0	1	1	1
	T_b	1	1	0	1	1	0
	T_c	1	1	1	1	0	0

2.4 Timing Sequence of the current Control

Fig. 2 shows the timing sequence of the current controller. The kth interrupt signal generated by the PWM generator starts the control process, as shown in Fig. 2(a). Synchronized with this interrupt signal, the AD converter samples the required values such as phase currents, dc link voltage, and rotor position to calculate the output voltages at the same time The gray section show in Fig. 2(b) represents the duration of the calculation time for the current control. The output value of the current controller is uploaded into the PWM generator using the signal, as shown in Fig. 2(c). During the (k+1)th period of the current control process, the phase voltages calculated in the previous period are applied to the motor through the inverter, as shown in Fig. 2(d). The resultant phase currents are sensed, using the (k+2)th interrupt signal, as shown in Fig. 2(e).

From the starting time of the current control to the sensing time of the resultant phase currents, there are not one, but two sampling period delays.

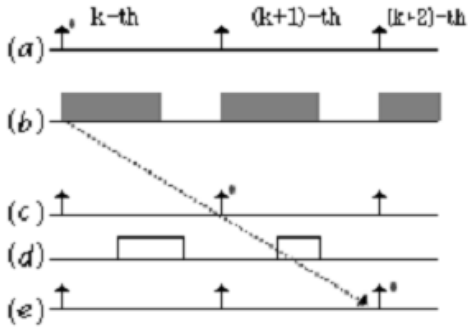

Fig. 3 Timing Sequence of current controller

2.5 The Conventional Predictive Current Controller

In a conventional predictive current controller, the control voltages which produce the required stator currents can be calculated using (3) and (4) as

$$V_{qs}^*(k) = R_s i_{qs}(k) + L_q \frac{i_{qs}^*(k+1) - i_{qs}(k)}{T_s} + w_r L_d i_{ds}(k) + w_r \lambda_{PM} \quad (10)$$

$$V_{ds}^*(k) = R_s i_{ds}(k) + L_d \frac{i_{ds}^*(k+1) - i_{ds}(k)}{T_s} - w_r L_q i_{qs}(k) \quad (11)$$

where $i_{qs}^*(k+1)$ and $i_{ds}^*(k+1)$ are the reference current values at the $(k+1)th$ sampling time. The conventional predictive current controller is a kind of high gain controller if the rotor speed and the back EMF terms are known and compensated properly.

Fig. 4 shows the simulation results for the current dynamics of the conventional predictive current control implemented in the full digital system. The current command is changed at the peak of the phase current when the rotor speed is about 1500 rpm. Since one more period is needed for the control calculation in the system than is expected, a large overshoot and oscillation have been observed when the current command in the -axis is changed from -1 A to 1 A.

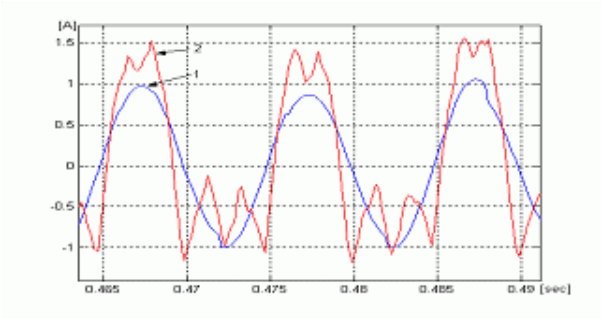

Fig. 4 wave of conventional Predictive Current Control

2.6 Proposed Predictive Current Controller

2.6.1 The Proposed Current Controller

This paper proposed the novel predictive current control in order to solve that the conventional predictive current control method generate the overshoot and oscillation. If we adjust the equation (10) and (11) of the voltage equation of the conventional predictive current control for PMSM, the adjusted voltage equation can be expressed as

$$V_{qs}(k) = Ai_{qs}(k) + Bi_{qs}(k+1)L_d\omega_r(k)i_{ds}(k) + \lambda_{PM}\omega_r(k) \quad (12)$$

$$V_{ds}(k) = Ai_{ds}(k) + Bi_{ds}(k+1) - L_q\omega_r(k)i_{ds}(k) \quad (13)$$

Where, $A = R_s - L_s/T_s$, $B = L_s/T_s$

During the (k+1)th period, as shown in Fig. 2(d), the PMSM was operated by the control voltage V(k+1) which is calculated during the (k)th period.

$$V_{qs}(k+1) = Ai_{qs}(k+1) + Bi_{qs}(k+2) + L_d\omega_r(k+1)i_{ds}(k+1) + \lambda_{PM}\omega_r(k+1) \quad (14)$$

$$V_{ds}(k+1) = Ai_{ds}(k+1) + BI_{ds}(k+2) - L_q\omega_r(k+1)i_{qs}(k+1) \quad (15)$$

For the regulation of the current, $i_{qs}(k+2)$ and $i_{ds}(k+2)$ can be considered as the desired current. And, in the equation (14) and (15), terms, which is from third term to last term, is values which generated by real PMSM.
therefore, during the (k+1)th period, the control output voltage $V_{dq}^*(k+1)$, which is applied in the PMSM, can be expressed as.

$$V_{qs}^*(k+1) = Ai_{qs}(k+1) + Bi_{qs}^*(k+2) + L_d\omega_r(k+1)i_{ds}(k+1) + \lambda_{PM}\omega_r(k+1) \quad (16)$$

$$V_{ds}^*(k+1) = Ai_{ds}(k+1) + Bi_{ds}^*(k+2) - L_q\omega_r(k+1)i_{qs}(k+1) \quad (17)$$

Here, $i_{dq}^*(k+2)$ and $V_{dq}^*(k+2)$ is the reference current and voltage of the sampling moment. From equation (16) and (17), the method, which can solve the $i_{dq}(k+1)$, and $i_{dq}^*(k+2)$, $w_r(k+1)$ is from 4.2 to 4.4

4.2 Compensation of the difference speed and position

The Compensation of the difference speed and position is a half of difference between kthy and (k+1)th of the speed and position. The difference of the speed and position is very small because as the very small time of the sampling time.
And, the compensate value is optimal value by simulation
Therefor, the compensation of the difference speed and position can be expressed as

4.3 The value of the $\tilde{i}_{dq}(k+1)$

The moment, which come out from the speed controller, is fast as one step than the moment which is generated from PMSM
Therefore, $V_{dq}^*(k-1)$ and $\tilde{V}_{qs}(k)$ is same. Here, $\tilde{V}_{qs}(k)$ is the q-axis voltage estimated in the kth.

Table 2. Compensation of the difference speed and position

	Kth -(k-1)th <0	Kth – (k-1)th > 0
w_{comp}	$-\frac{w_r(k)-w_r(k-1)}{2}$	$\frac{w_r(k)-w_r(k-1)}{2}$
θ_{comp}	$-\frac{\theta_r(k)-\theta_r(k-1)}{2}$	$\frac{\theta_r(k)-\theta_r(k-1)}{2}$

The value of the $V_{qs}^*(k-1)$ and $\tilde{V}_{qs}(k)$ can be expressed as equation (18) and (19), from the voltage equation of PMSM

$$V_{qs}^*(k-1) = Ai_{qs}^*(k-1) + Bi_{qs}^*(k) + L_d\omega_r(k)i_{ds}(k) + \lambda_{PM}\omega_r(k) \quad (18)$$

$$\overline{V}_{qs}(k) = Ai_{qs}(k) + Bi_{qs}(k+1) + L_d\omega_r(k)i_{ds}(k) + \lambda_{PM}\omega_r(k) \quad (19)$$

If we subtract the equation (18) from equation (19), we can know the difference voltage value of the moment of kth

$$V_{qs}^*(k-1) - \overline{V}_{qs}(k) = A\{i_{qs}^*(k-1) - i_{qs}(k)\} + B\{i_{qs}^*(k) - i_{qs}(k+1)\} \quad (20)$$

We can consider as $V_{qs}^*(k-1) - \tilde{V}_{qs}(k) = 0$ in order to know $i_{qs}^*(k+1)$ which make the difference voltage as 'o' in equation (20), If we adjust this, this can be expressed as.

$$\tilde{i}_{qs}(k+1) = \frac{A}{B}\{i_{qs}^*(k-1) - i_{qs}(k)\} + i_{qs}^*(k) \quad (21)$$

We can solve the $\tilde{i}_{ds}(k+1)$ as the course of the $\tilde{i}_{qs}(k+1)$.

$$\tilde{i}_{ds}(k+1) = \frac{A}{B}\{i_{ds}^*(k-1) - i_{ds}(k)\} + i_{ds}^*(k) \quad (22)$$

Here, $\tilde{i}_{ds}(k+1)$ and $\tilde{i}_{qs}(k+1)$ is the current value of (k+1)th moment

4.4 The value of the $i_{dq}^*(k+2)$

The values of the $i_{qs}^*(k+1)$ and $i_{ds}^*(k+1)$ can obtain using the increment matrix C. The increment matrix C is expressed as equation (23)

$$C = \begin{bmatrix} \cos(\omega(k)T_s) & \sin(\omega(k)T_s) \\ -\sin(\omega(k)T_s) & \cos(\omega(k)T_s) \end{bmatrix} \quad (23)$$

Here, we must apply the $w_r(k+1)$ because of obtaining the reference current of (k+1)th moment
If we arrange using this, the reference current $i_{dq}^*(k+1)$ of the (k+1)th moment can be expressed as

$$i_{qs}^{*}(k+1) = \cos((\omega_r(k)+\omega_{comp})T_{si})i_{qs}^{*}(k) + \sin((\omega_r(k)+\omega_{comp})T_{si})i_{ds}^{*}(k) \quad (24)$$

$$i_{ds}^{*}(k+1) = -\sin((\omega_s(k)+\omega_{comp})T_{si})i_{qs}^{*}(k) + \cos((\omega_r(k)+\omega_{comp})T_{si})i_{ds}^{*}(k) \quad (25)$$

4.5 Voltage limitation

After the voltage command $V_{dq}^{*}(k+1)$ is calculated in (16) and (17), there is a question as to whether the magnitude of the corresponding voltage space vector is beyond the actual voltage limitation or not. If this magnitude is greater than the maximum available inverter output voltage, the control voltages should be adjusted. Otherwise the correct voltage command for the next period cannot be obtained since the applied voltage is different from the calculated one. The adjusted voltages $V_{dq}^{**}(k+1)$ can be obtained from the command voltages $V_{dq}^{*}(k+1)$ as

$$v_q^{**}(k) = v_q^{*}(k)\frac{V_{dc}}{\sqrt{3}V_s} \quad (26)$$

$$v_d^{**}(k) = v_d^{*}(k)\frac{V_{dc}}{\sqrt{3}V_s} \quad (27)$$

Here, $V_s = \sqrt{V_{qs}^{*} + V_{ds}^{*}}$

Table 3. Rating and Parameters of the PMSM

ITems	Value
Rated Power	2.2 Kw
Rated Speed	2000rpm
R_s	0.1246 Ω
L_s	1.3441 mH
Pole pair	4

5. Simulation

The performance of the proposed current scheme has been analyzed by simulation using the actual parameters of 2.2Kw PMSM drive with the assumptions as follows: no saturation in flux linkage, sinusoidal EMF's, and constant speed during a sampling period. The Visual C++ language program is used in the simulation. The dc link voltage, which is assumed to be ideal, equal 220V. The ratings and parameter values of the PMSM are listed in the Table 3. In the simulation, the inverter switches are considered as ideal, I.e., zero conduction voltage drop and zero commutation time. The sampling period is 150 μs. The dynamic performance of the proposed current controller has been studied by considering the whole system.

In the Fig. 5(a), the d-axis reference current i_d^{*} is '0' and the q-axis reference current change from 3A to -3A at the moment of 0.3 second. In the Fig. 5(b), the d-axis reference current i_{ds}^{*} is '0' and the q-axis reference current change from -3A to 3A at the moment of 0.3 second. And, in Fig 5(c) and Fig. 5(d), the q-axis reference current change from 30A to -30A at the moment of 0.3 second. When the reference speed change 1000rpm at 0sec, and -1500rpm at 0.2sec, 1500rpm at 0.4sec, -1000rpm at 0.6sec, 1000rpm at 0.8sec, Fig. 6 is the measured speed track the reference speed

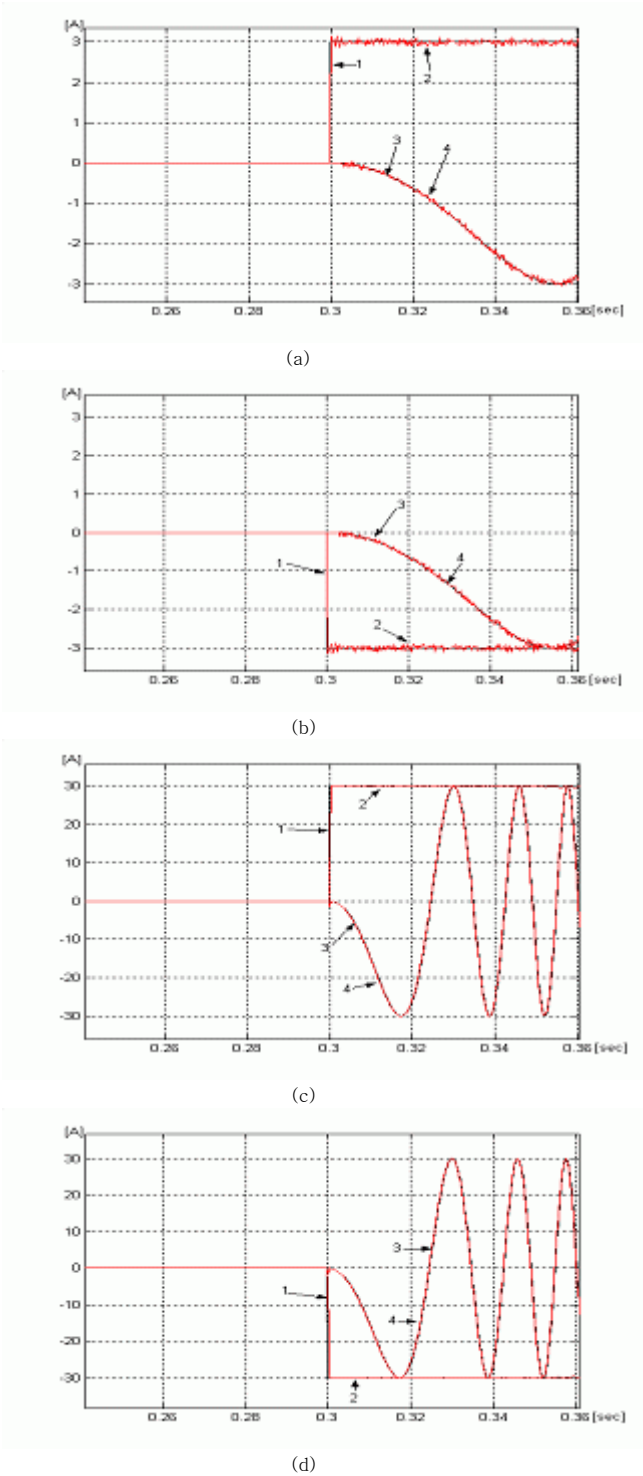

(a) (b) (c) (d)

Fig. 5 Current response of the proposed current control
1: q-axis current command, 2: q-axis current response
3: a-phase current command, 4: a-phase current response

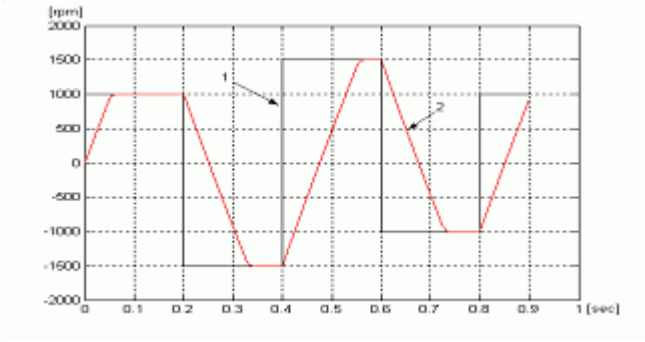

(a)

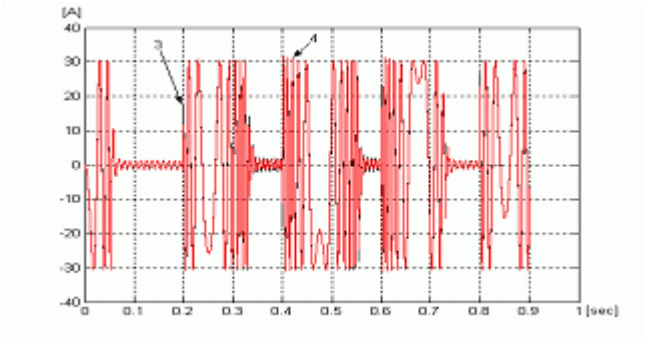

(b)

Fig. 6 response of the whole system with fast speed chang
1: speed command, 2: speed response,
3: a-phase current command, 4: a-phase current response

6. Conclusion

This paper presents a novel predictive current control method for a PMSM that considers the finite calculation delay of control devices. the conventional predictive current controller is hard to implement in the full digital current controller since a finite calculation time causes a delay between the current sensing time and the time it takes to apply the voltage to the motor. By modifying a conventional predictive current controller that considers the calculation delay, there is a large improvement in the current control performance in the both transient and steady states.

ACKNOELEDGEMENT

This work was supported by the National Research Laboratory Program of the Korean Ministry of science & Technology (MOST).

REFERENCES

[1] H. T. Moon, H. S. Kim, and M. J. Youn, "A Discrete-Time Predictive Current Control for PMSM," *IEEE Trans. on Power Electronics*, Vol. 18, No. 1, pp. 464-472, 2003.

[2] M. A. Rahman, "Analysis of Current Controllers for Voltage-Source Inverter," *IEEE Trans. on Industrial Electronics*, Vol. 44, No. 4, pp. 477-485, 1997.

[3] O. Kurker, "Discrete-Time Current Control of Voltage-Fed Three-Phase PWM Inverters," *IEEE Trans. on Power Electronics*, Vol. 11, No. 2, pp. 260-269, 1996.

[4] C. E. Miller, et. al., "Modelling A Permanent Magnet Linear Synchronous Motor for Control Purpose," *IEEE Africa 2002*, pp. 671-674, 2002.

[5] Young Soo Seo and Young Jin Kim, "Vector Control of Inductor Motor for estimating Back-EMF of Hyperstable MRAS," *Journal of Research Institute of Industrial Technology*, Vol. 20. pp. 727-732, 2001.

[6] In-Hwan Oh, Gun-Woo Moon, Sung-kwun Kim, "A Novel Predictive Current Control Induction Motor Using Resonant DC Link Inverter," *IEEE*, pp. 1106-1111, 1996.

[7] Li Zhen and Longya Xu, "Sensorless Field Orientation Control of Induction Machines Based on a Mutual MRAS Scheme," *IEEE Trans. on Industrial Electronics*, Vol. 45, No. 5, October 1998.

[8] Seung-Gi Jeong and Myung-Ho Woo, "DSP-Based Active Power Filter with Predictive Current Control," *IEEE Trans. on Industrial Electronics*, Vol. 44, No. 3, June 1997.